DOI: 10.5137/1019-5149.JTN.21931-17.2
Received: 30.10.2017 / Accepted: 09.01.2018
Published Online: 28.02.2018

Turk Neurosurg, 2018

Original Investigation

Spinal Peripheral Primitive Neuroectodermal Tumors: A Radiological Analysis of Ten Cases

Xiaoping YI[1,2], Moling ZHOU[1], Shenghui LIAO[3], Guanghui GONG[4], Hongling YIN[4], Yongheng CHEN[5], Weihua LIAO[1]

[1]Central South University, Xiangya Hospital, Department of Radiology, Changsha, Hunan Province, China
[2]Central South University, Xiangya Hospital, Postdoctoral Research Workstation of Pathology and Pathophysiology, Basic Medical Sciences, Changsha, Hunan Province, China
[3]Central South University, School of Information Science and Engineering, Changsha, Hunan Province, China
[4]Central South University, Xiangya Hospital, Department of Pathology, Changsha, Hunan Province, China
[5]Central South University, Xiangya Hospital, Key Laboratory of Cancer Proteomics of Chinese Ministry of Health, Changsha, Hunan Province, China

ABSTRACT

AIM: To summarize the imaging features of spinal peripheral primitive neuroectodermal tumor (spPNET) patients.

MATERIAL and METHODS: The computed tomography and magnetic resonance imaging features of 10 spPNET patients, four men and six women, were retrospectively analyzed, and their clinicopathological data were reviewed.

RESULTS: The mean age of the patients was 24.7 years (range, 3-44 years). Ten spPNET lesions were found in the ten patients, including six extradural and four intradural extramedullary lesions. Radiologically, spPNET typically presented as heterogeneous isointense lesions with a heterogeneously enhanced pattern. A "vault wall-like growth" pattern, a linear enhancement pattern, and vertebral bone involvement tended to be found in the extradural lesions, whereas a ring enhancement pattern was found in the extramedullary intradural lesions. Positive Ki-67 expression might be related to necrosis, bone destruction, and hemorrhage.

CONCLUSION: A well-defined spinal mass showing isointensity/attenuation with heterogeneous enhancement accompanied by other imaging features may be suggestive of spPNET and should be added to the list of differential diagnosis.

KEYWORDS: Computed tomography, Diagnosis, Magnetic resonance imaging, Primitive neuroectodermal tumor, Spinal peripheral

INTRODUCTION

Primitive neuroectodermal tumors (PNETs) are poorly differentiated malignant tumors comprising small round cells of neuroectodermal origin that occur primarily in children and adolescents (17-19). PNETs can be further classified into two types based on their anatomical location: central primary neuroectodermal tumors (cPNETs) and histologically similar peripheral primitive neuroectodermal tumors (pPNETs)(16). Although PNETs can theoretically occur in any part of the body (1,6,17,22), they are most commonly found in brain parenchyma, especially in the frontal lobe, with rare reports in the spinal region. Due to the extensive application of immunohistochemistry (IHC) and various imaging techniques, the number of reported PNETs has gradually increased over recent years. Nonetheless, primary spinal peripheral PNETs (spPNETs) remain rare. Most of the studies to date investigating spPNETs have focused on their clinicopathological features as well as on the treatment and prognosis of this rare disease. Conversely, only a few studies have reported imaging findings associated with spPNETs; moreover, the results are non-specific and limited, which precludes meaningful summarization (1,3-8,13-15,17,18,21).

qr code

Corresponding author: Moling ZHOU
E-mail: doctorzhoumoling@163.com

Notably, spPNETs generally share similar imaging features with other spinal tumors, such as lymphoma and schwannoma, and accordingly, spPNETs are frequently misdiagnosed as other tumors.

Although there is no consensus thus far, as the understanding of pPNETs has recently and gradually deepened, the treatment strategy for this disease has changed to a comprehensive modality that involves surgery, neo-adjuvant/adjuvant radio- or chemotherapy. Of particular and growing concern is that the role that preoperative neo-adjuvant chemo-/radiotherapy plays in the treatment of this disease (2). As this treatment modality might provide the greatest therapeutic benefit to patients with spPNETs, it is important to obtain a precise preoperative diagnosis of the disease via combined analysis of radiographic and clinical data.

The present study retrospectively summarizes the imaging findings of ten patients with spPNETs while focusing on morphological, texture and enhancement characteristics in an attempt to correlate these characteristics with the pathological features of spPNETs to deepen our understanding of this rare disease.

MATERIAL and METHODS

Design and Patients

This study was conducted in accordance with the Declaration of Helsinki and all of its amendments as well as national regulations.

We searched the pathologic and medical record database to identify patients with surgically and pathologically confirmed spPNET in our hospital between July 2002 and July 2009. Patients without complete medical records, radiographic data or prognosis data were excluded. Ultimately, data for ten patients with spPNET were included in this study. Of these patients, three had undergone complete computed tomography (CT) scans, and nine had undergone magnetic resonance imaging (MRI) examinations. Clinical and radiological data were collected.

Imaging Techniques

MRI scans were obtained using a 1.5-T superconductive unit (Gyroscan Intera, Philips Medical Systems, Batadorp, Eindhoven, The Netherlands); a synergy spine coil was also used. The imaging sequences were as follows: spin-echo T1-weighted and T2-weighted sequences with or without fat suppression and contrast-enhanced spin-echo T1-weighted sequences with fat suppression obtained along the sagittal, coronal, and transverse planes. The CT scans were performed using a 64-slice spiral CT (Sensation64, Siemens AG, Forchheim, Germany). The scan parameters were as follows: 5-mm section thickness, 1-mm slice thickness reconstructions, 120 kV, 90 to 270 mA, and a 256×256 matrix. A 100-mL intravenous bolus dose of a non-ionic iodinated contrast agent (iopromide; Ultravist; Schering AG, Berlin, Germany) was administered at a rate of 3-4 mL/s.

Imaging Analysis

Two experienced radiologists specializing in nervous system diseases for more than ten years, who were blinded to the previous clinical radiological and histopathological results, independently reviewed all images. The final assessment of the findings was reached via consensus. The MRI or CT scans were evaluated and analyzed for the following parameters: vertebral level of involvement (cervical, thoracic, lumbar, or sacral), tumor location (intramedullary, extramedullary intradural, or extradural), size, morphology ("drilling hole" or "vault wall-like growth" patterns), margin (well-defined or ill-defined), lesion texture (homogeneous or heterogeneous; with or without necrosis; hemorrhage or calcification), signal intensity and CT density (hypo-, iso- or hyperintense in relation to the paraspinal muscle signals), contrast enhancement characteristics (homogeneous or heterogeneous), the presence of paraspinal tissue masses, and vertebral or other bony changes.

A "drilling hole" pattern was defined as the tendency to extend through the intervertebral foramen. A "vault wall-like growth" pattern was defined as encroachment along the spinal canal over multiple vertebral segments (11).

Pathological Analysis

Two experienced pathologists specializing in nervous system diseases for more than ten years independently performed pathological re-analysis of all spPNET cases, and the findings were recorded via consensus. Hematoxylin and eosin (H&E) and IHC staining procedures were performed for all cases. Expression of neuron-specific enolase (NSE), CD99, CD3, CD26, CD30, CD34, CD56, S-100, glial fibrillary acidic protein (GFAP), cytokeratin (CK), synaptophysin (Syn), leukocyte common antigen (LCA), chromogranin A (CgA), vimentin, Ki-67, terminal deoxynucleotidyl transferase (TdT), myogenin, and myeloperoxidase (MPO) was examined.

RESULTS

Four men and six women with a mean age of 24.7 years (range, 3-44 years) participated in the study. The presenting symptoms included local back pain in four patients, numbness in the lower extremities in five patients, radiating pain in the lower limb in three patients and radiating pain in the left upper limb in one patient. None of the patients had significant medical histories. A total of ten lesions were found near the spinal column in the ten patients. Lesions were found in the cervical, thoracic, or lumbar spines or in the lumbosacrum or sacrum. Among these locations, the sacrum was the site most commonly involved (5/10, 50%; Table I). The detailed clinical findings of ten patients are shown in Supplementary Table I.

Six of ten patients had extradural lesions. Of these six lesions, five extended through the intervertebral foramen into paraspinal regions, including two that formed a large ill-defined paraspinal soft tissue mass. Four lesions showed a "vault wall-like growth" pattern. The size of the lesions varied from 2.6 to 7.2 cm (mean, 6.2 cm). Five lesions were well defined, whereas one was ill-defined masses (Table I).

All lesions exhibited heterogeneous iso- or hypointense signals on T1-weighted images (T1-WI), which were correlated with heterogeneous hyperintense signals on T2-weighted images (T2-WI) (Figure 1A-H). Necrosis was found in two lesions. All lesions were heterogeneously enhanced after administration of the contrast agent. Three lesions displayed a clearer linear enhancement pattern than the remaining three lesions, which showed homogeneous enhancement (Figure 2A-F). Vertebral or bony involvement was observed in four patients, and one patient had a paraspinal mass encasing paraspinal blood vessels. In one patient, the vertebral body was collapsed.

Four patients presented with intradural extramedullary lesions. Two lesions extended into the paraspinal region through the intervertebral foramen, without formation of a large, ill-defined paraspinal soft tissue mass. Notably, one mass exhibited a "vault wall-like growth" pattern, but the remainder did not display similar patterns. Lesion size varied from 1.4-3.5 cm (mean, 2.45 cm), and all masses were well defined. The signal intensity was similar to the intensity of the extradural lesions mentioned above except with regard to one lesion, which showed a hyperintense signal on T1-weighted images and a hypointense signal on T2-weighted images because of hemorrhage. These lesions were also heterogeneously enhanced after administration of the contrast agent. Interestingly, one lesion was almost completely necrotic, except for its edge. Two intradural extramedullary lesions presented with ring enhancement, as large areas of their centers were occupied by hemorrhage and necrosis. A thickened and obviously enhanced dural theca was present in one patient. Only one patient with obvious necrosis had vertebral or bony involvement.

Most lesions appeared on CT as heterogeneous isodense masses with a homogeneous enhancement pattern. A heterogeneous enhancement pattern was observed when obvious necrosis was present (Figures 1A-H, 3A-H).

No obvious calcification or cystic degeneration was found. The

Table I: Clinical Data and Main Radiological Findings in 10 Patients with spPNET

	All	Intradural, extramedullary	Extradural
Case	10	4	6
Mean age (years)	24.7	17	27
Sex			
M	4	3	1
F	6	1	5
Location		Cervical spine (1); Thoracic (1); Sacrum (2)	Thoracic (1); Lumbar (2); Sacrum (3)
Size (cm)	4.3	2.45	6.2
Margin			
Well-defined		4 (100%)	5 (83%)
Ill-defined		0 (25%)	1 (17%)
Morphology			
Extending through the neural foramina	7	2 (50%)	5 (83.3%)
Vault-wall-like	5	1 (25%)	4 (66.7%)
Necrosis		1 (25%)	1 (16.7%)
Hemorrhage		1 (25%)	0
Cyst		0	0
Calcification		0	0
Enhancement			
Homogenous		1 (25%)	2 (33.3%)
Heterogeneous		3 (75%)	4 (66.7%)
Ring enhancement		2 (50%)	0
Linear enhancement pattern		0	3 (50%)

M: *Male,* ***F:*** *Female.*

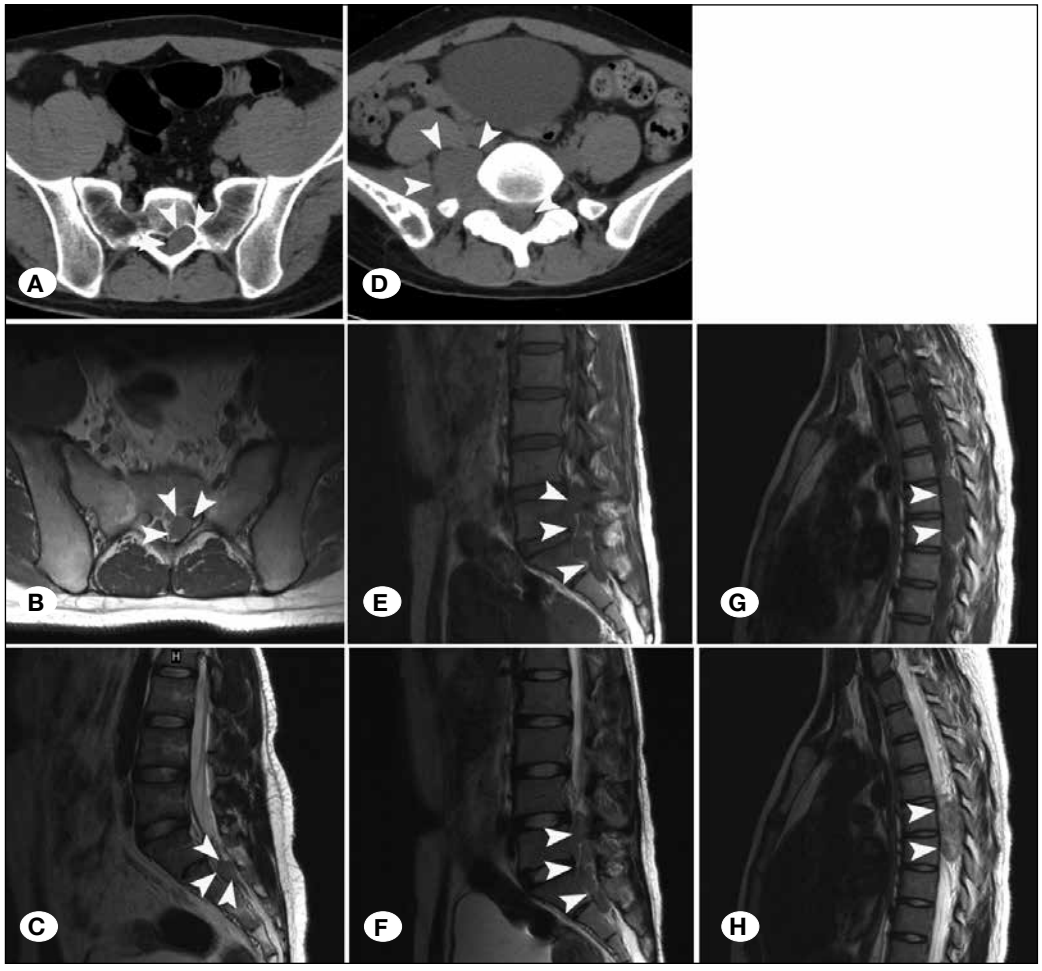

Figure 1: A) spPNET mass usually presents as an iso-dense mass on CT, an isointense signal on T1-WI, and a heterogeneous hyperintense signal on T2-WI. **A, B, C)** One extradural lesion (Case 2) at the S1 vertebral level (arrowheads). **D, E, F)** One intradural extramedullary lesion (Case 3) at the L5-S2 vertebral level (arrowheads). **G, H)** One extradural lesion (Case 1) at the T6-7 vertebral level (arrowheads).

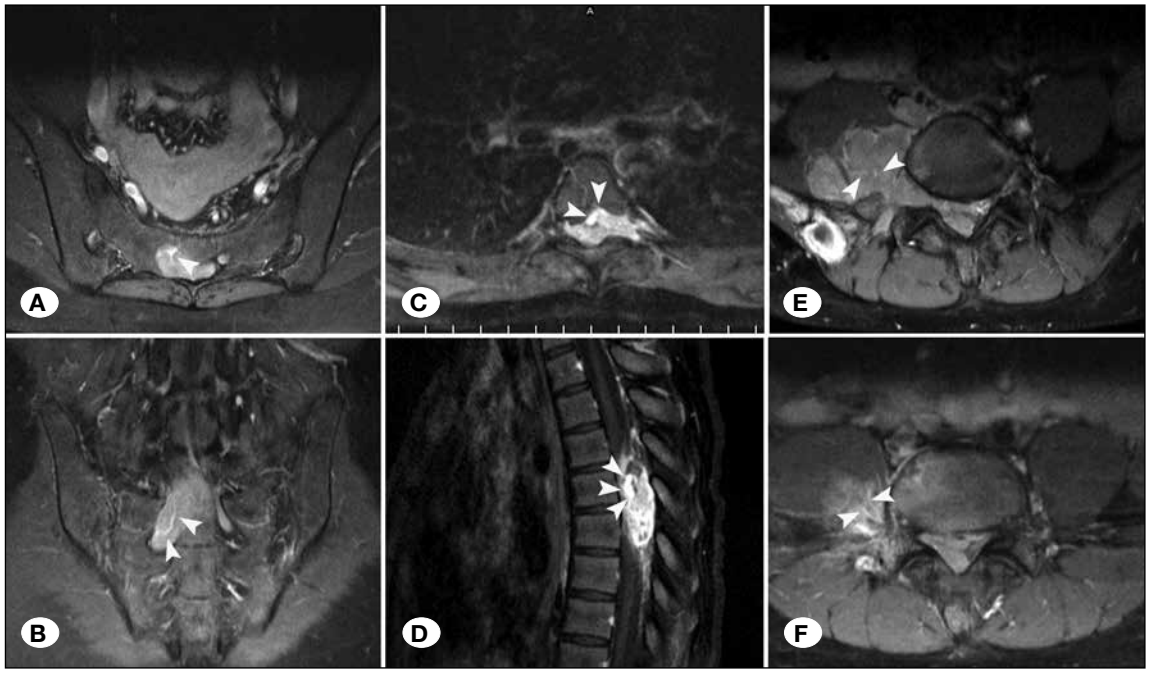

Figure 2: Post-contrasted T1-WI of three masses **(A, B; C, D** intradural extramedullary masses; **E, F** extradural mass) show a more obvious linear enhancement pattern (feeding artery, arrowheads) at the S1-2 (Case 8), T6-7 (Case 1) and L5-S2 (Case 3) vertebral levels, respectively, with three large ill-defined paraspinal soft tissue mass formed.

spinal cord or cauda equina was compressed in all patients. The detailed MRI and CT findings for these ten patients, and spPNET patients published in the English literature are shown in Supplementary Table 2 and Tables, respectively.

The treatment modalities included gross total resection (GTR) in six patients (60.0%) and subtotal resection (STR) in four patients (40.0%). All but one patient accepted adjuvant chemotherapy with vincristine, adriamycin, cyclophosphamide (VAC) or vincristine, ifosfamide, doxorubicin, and etoposide (VIDE) protocols, and the radiotherapy dose ranged from 30-50 Gy. Intraoperative STR failure was usually related to the presence of ill-defined margins and a "vault wall-like growth" mass pattern. No biopsy or neo-adjuvant chemotherapy was performed. The prognosis of the ten patients was extremely poor, with a median survival time of 27.4±5.2 months; the overall 1-year survival rate was 90.0% (3/10), and the 2-year survival rate was 40.0%. Treatment and prognosis details can be found in Supplementary Table 1. In addition, patients who underwent GTR (median survival time, 35.2±6.8 months) survived longer than those who underwent STR (15.8±3.6 months) ($p<0.05$) (Figure 4A,B).

Histologically, tumors were found to be predominately composed of numerous small, dense and round cells, with scattered interstitial components. Homer-Wright rosettes were observed in two lesions. IHC examination revealed consistent positive staining for CD99 in the tumors of nine patients, but negative staining in the remaining patient. NSE and Syn were both expressed in the lesions of three patients. IHC with anti-MIB-1 (Ki-67) antibodies revealed an elevated proliferation index in four cases (range, 10-80%). Vimentin staining was positive in five cases. Fluorescent in situ hybridization (FISH) and chromosomal analyses were not performed in this series. The detailed IHC characteristics of the lesions are shown in Table III.

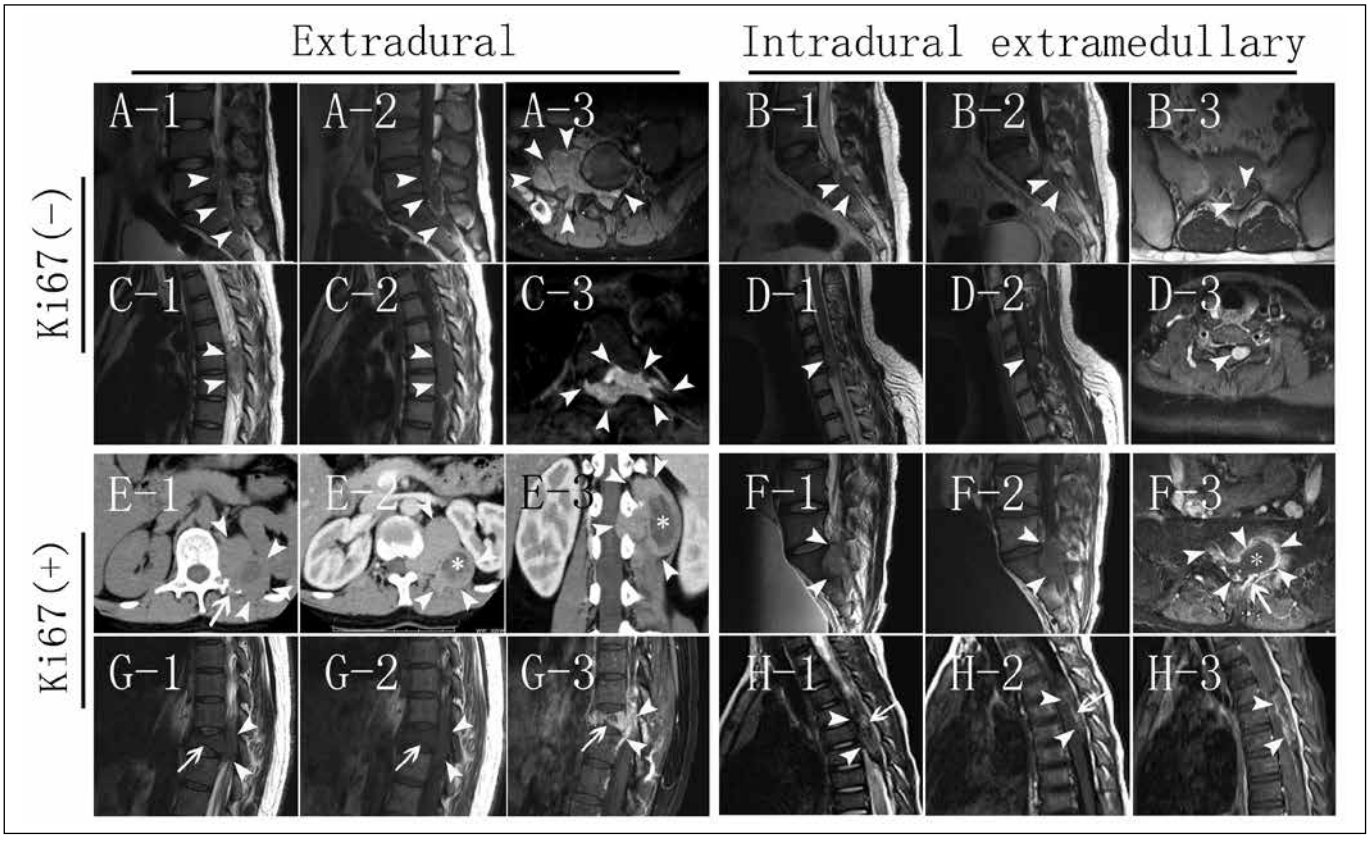

Figure 3: Significant differences of extradural and intradural extramedullary spPNET. (**A.** Case 3; **C.** Case 1; **E.** Case 4; **G.** Case 6) Images of four extradural masses (CT of one patient and MRIs of three patients)(arrowheads). Three masses **(A, C, E)** were relatively large, and two masses **(A, E)** formed an asymmetrical paraspinal soft tissue mass. Three masses **(A, C, G)** exhibited a "vault wall-like growth" pattern (arrowheads). Two masses (**E, G**) showed bone destruction (arrow). (**B.** Case 2; **D.** Case 5; **F.** Case 9; **H.** Case 10) MRIs of four patients with intradural extramedullary masses (arrowheads). Three masses **(B, D, F)** were relatively small. No asymmetrical paraspinal soft tissue mass formation was observed, and none exhibited a "vault wall-like growth" pattern, except for the mass shown in **F**. Five masses showed an obvious "drilling hole" pattern **(A, C, D, E, F).**
Significant differences for Ki-67(-) and Ki-67(+) masses of spPNET. (**A**. Case 3; **B.** Case 2; **C**. Case 1; **D.** Case 5) MRIs of four patients with negative Ki-67 expression. None exhibited vertebral or other bone destruction, necrosis, or hemorrhage. **(E.** Case 4; **F.** Case 9; **G.** Case 6; **H.** Case 10) Four masses (CT of one patient and MRIs of three patients) with positive Ki-67 expression. Three masses **(E, F, G)** showed vertebral or other bone destruction (arrow) and necrosis (**E F**, asterisk). The remaining mass **(H)** showed obvious hemorrhage (arrow).

Table II: Summary of sPNET Patients Reported in the English Literatures (Focus on Radiological Features)

Reference	Type	Number of patients	Gender (male/ female)	Age (mean, years)	Method obtained pathological diagnosis	T1- WI	T2- WI	T1- WI C+	Leptomeningeal enhancement (cases)	Vertebral collapse/ destruction (cases)	Paraspinal mass (cases)	Cyst (cases)	Hemorrhage (cases)	Calcification (cases)
Wu et al. (21)	Clinical Trial	7	3/4	26.3	Resection	Hypointense or Isointense	Hyperintense	Heterogeneous	1	1	2	-	-	-
Duan et al. (3)	Clinical Trial	6	5/1	19	Resection	Hypointense or Isointense	Hyperintense	Heterogeneous	2	4	4	-	-	-
Qi et al. (16)	Clinical Trial (focused on the clinico-pathological features)	25	9/16	20	Resection	No depict	No depict	No depict	No depict	No depict	No depict	No depict	No depict	No depict
Hung et al. (8)	Case report	5	2/3	9	Image-guided biopsy or resection	Hypointense or Isointense	Hyperintense or Isointense	Heterogeneous	No	4		2	1	-
Thoriya et al. (18)	Case report	1	0/1	31	Resection	Isointense	Hyperintense	Heterogeneous	No	-	-	+	-	-
Hrabálek et al. (7)	Case report	1	1/0	29	Resection	Isointense	Hyperintense	Heterogeneous	No	-	+	-	-	-
Jain et al. (9)	Case report	1	0/1	54	Resection	Iso-, Hypointense	Hyperintense	Heterogeneous	No	-	-	-	No depict	No depict
Jingyu et al. (10)	Clinical Trial (focused on the clinico-pathological features)	4	3/1	26	Resection	Hypointense or Isointense	Hyperintense	No depict	No depict	No depict	No depict	No depict	No depict	No depict

Interestingly, among the four cases with positive Ki-67 staining, two extradural lesions were accompanied by obvious necrosis and bone destruction. The remaining two intradural extramedullary lesions displayed hemorrhage and massive necrosis, with both exhibiting a "ring-enhancement" pattern (Figure 3A-H).

DISCUSSION

Diagnoses of spPNET are extremely rare. This condition has been associated with adult onset, and male predominance has been reported (10). Nonetheless, six female (60%) and four male (40%) patients were included in our case series; moreover, the mean age of presentation was 24.7 years (range, 3-44 years), which is not consistent with earlier reports. The majority of the lesions in our patients appeared to easily infiltrate the paraspinal region through the neural foramen; thus, corresponding symptoms of numbness and radiating pain in the limbs due to oppression of the lesions were common, as also demonstrated in previous studies.

Table III: Immunohistochemistry Characteristics of Ten spPNETs

Case No.	Positive	Negative
1	CD99, CD56, NSE, Syn	TdT, desmin, CD3, CD20, PAX-5, TdT, CgA, CK-Pan
2	CD99, CD56, NSE, Syn	CK, CD3, CgA, actin, CD20, PAX-5, TdT, desmin
3	CD99, CD56, vimentin, P53, Ki67 (80%), FLI-1	Syn, CgA, TIF-1, CK7, CK-Pan, S-100, desmin
4	CD99, Ki67 (A few+), vimentin	CD56, GFAP, NSE, Syn, CgA, S-100, CD34, LCA, PAX-5, TdT, MPO NeuN
5	CD99, CK-Pan, Ki67 (10%), LCA, MPO	CD56, GFAP, Syn, CgA, Myoglobin, NF-Pan, PAX-5, TdT, S-100, NeuN
6	CD56, Ki67 (25%), LCA, NSE, Syn, CD45RO CgA	CK-H, CK-L, CK-Pan, EMA, S-100, Vimentin, CD20, TIF-1, Myoglobin, Melan-A
7	CD56, CD99, vimentin, NSE	CD57, CgA, EMA, S-100, Syn, CD45RO, LCA, PAX-5, TdT
8	CD21, CD99	CD20, CD10, CD3, CD45RO, CD5, NSE, PAX-5, TdT
9	CD99, vimentin,	Syn, CgA, CK-L, CK-P, LCA, CD20, CD45RO, GFAP, S-100, HMB45,
10	CD99, vimentin, CD56, S-100 (Focal +)	Syn, CK-H, CK-L, CK-P, MBP, PSA, TIF-1

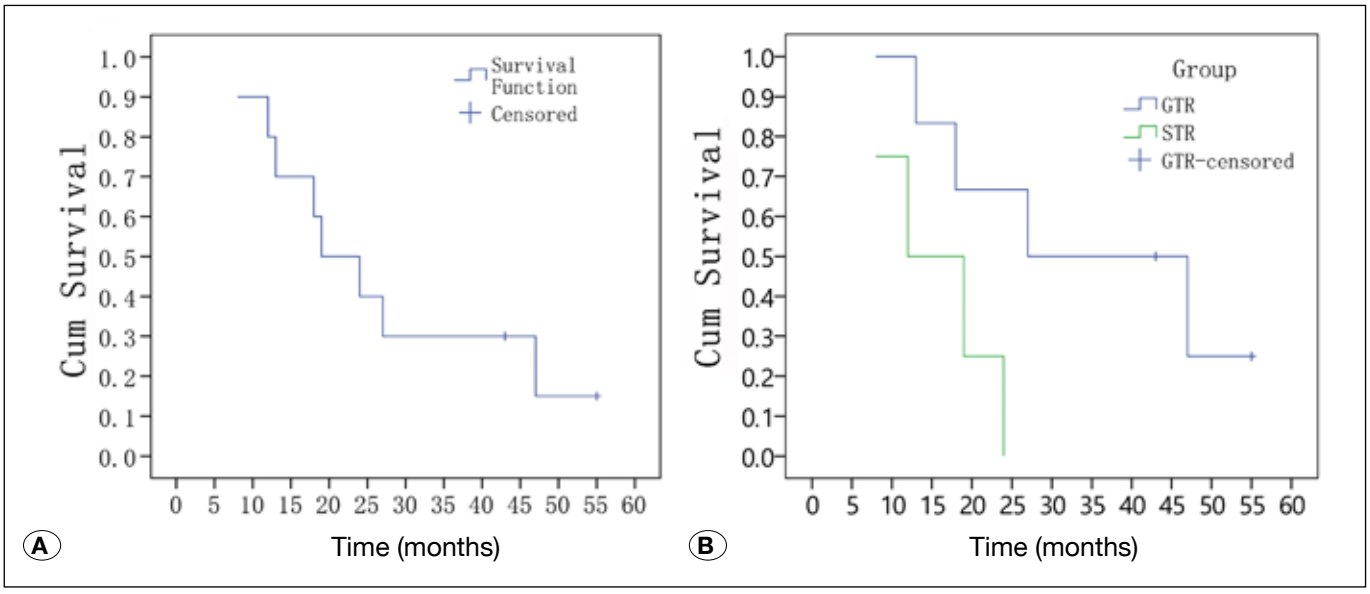

Figure 4: Kaplan-Meier curves for patients with spPNET. All patients (n=10) **(A).** The 10 patients were divided into two groups based on the surgical method used: gross total resection (GTR, n=6) or subtotal resection (STR, n=4) **(B).** Comparison between the two groups revealed significant differences ($p<0.05$).

Therefore, as it is extremely difficult to identify a patient with spPNET using these non-specific symptoms, diagnosis is largely dependent on imaging results.

Imaging techniques including MRI and CT play an important role in the diagnosis of patients with spinal tumors and in preoperative surgical planning (1,6,20). Unfortunately, definitive diagnosis of spPNET remains challenging for radiologists and clinicians. Furthermore, some researchers have recently suggested that neo-adjuvant therapies (e.g., preoperative radiotherapy, chemotherapy, or both) strongly improve the survival rates of patients with this extremely malignant disease by significantly increasing the radical resection rate of localized lesions and eliminating possible micro-metastases (2). Thus, accurate preoperative diagnosis of spPNETs is especially critical.

According to the previous limited reports of spPNET, the predominant location is the thoracolumbar level, with fewer cases in the sacral or cervical region (9). In addition, most spPNETs have been reported as well-defined masses. On MRI, spPNETs usually present as hypo- or isointense signals on T1-weighted images and hyperintense signals on T2-weighted images. By CT, spPNETs commonly appear as isodense masses that might be accompanied by hemorrhage and necrosis and a lack of calcification. After injection of the contrast agent, spPNETs tend to demonstrate a heterogeneous enhancement pattern (3,21). Moreover, intradural extramedullary lesions typically infiltrate the paraspinal tissues through the neural foramen and form a paraspinal soft tissue mass that has an asymmetrical size compared with its intraspinal component (3,7). Nevertheless, the literature to date regarding the radiological features of this rare disease is inadequate to enable distinguishing it from other common intraspinal tumors. Therefore, a reliable summary of spPNET imaging characteristics and their underlying pathological basis must be compiled and the findings discussed to deepen our understanding of the radiological features and potential clinicopathological foundation of this disease.

We observed other imaging findings in our series in addition to the radiological features mentioned above. First, the sacral level was the most common site in our study, a finding that differs from those of previous reports, in which the thoracolumbar level was more common (9). Second, previous publications have argued that extramedullary intradural spPNETs tend to extend through the intervertebral foramen and easily form a paraspinal soft tissue mass with an asymmetrical size compared with its spinal component (3). However, seven of the ten patients in our study exhibited not only intradural lesions but also extradural extramedullary lesions that tended to grow along the neural foramen. This finding suggests that the "drilling hole" pattern characteristic of this tumor is independent of its extradural or subdural location. Interestingly, only two patients with extradural spPNETs and none with extramedullary intradural spPNETs exhibited asymmetrical paraspinal soft tissue masses. We hypothesize that this result is due to the dura, which might play an important role in blocking the growth of the lesion through the intervertebral foramen. Importantly, the most common site in our series was at the sacral level, which has a longer neural foramen than the other spinal column levels; this difference inadvertently creates a relative barrier that hampers the growth of soft masses.

Third, awareness of the isointense signal characteristics of T1 images of tumors and the moderate density of CT images should be increased, which might help in differentiating spPNETs from most of the intraspinal tumors that often exhibit hypointense signals on T1-weighted images or hypoattenuation on CT images. Although this finding is not unique to this tumor, it might partially reflect its histological basis. As shown by H&E staining, spPNETs comprise numerous dense tumor cells combined with scattered interstitial tissue, which might be the pathological foundation of the radiological pattern.

According to previous studies, hemorrhage and necrosis are rare in spPNETs (8). Regardless, the present study identified hemorrhage or necrosis in four patients, though it is unclear how these phenomena occur or what they indicate. Interestingly, these events were more common in the Ki-67-positive cases in our series. Two extradural lesions were accompanied by necrosis and bone destruction; two intradural extramedullary lesions showed hemorrhage or massive necrosis and displayed a ring-enhancement pattern. Importantly, one of the two intradural extramedullary lesions with a Ki-67-positive rate of over 80% appeared as a mass that was almost entirely occupied by necrosis (except at its edge), with adjacent bone destruction. No obvious signs of necrosis or hemorrhage were found in the preoperative images of the four lesions with negative Ki-67 expression, except one that showed bone destruction. Thus, higher Ki-67 tumor indices might indicate greater likelihood of necrosis, hemorrhage, or bone destruction. In theory, the Ki-67 tumor index reflects tumor proliferation, and a tumor with a high Ki-67 index might grow too rapidly and exceed its blood supply, thereby leading to ischemia in some tumor cells and the subsequent occurrence of hemorrhage and necrosis. In addition, tumor cells with a higher Ki-67 index and proliferation ability might be more likely to be aggressive and to damage adjacent bones.

We also found a linear enhancement pattern in three extradural lesions; this might be a characteristic sign, and it has not been reported previously. This pattern might directly reflect the feeding artery in the tumor, which has been described as a nourishing blood vessel in other studies.

Based on our findings, intradural and extradural spPNET lesions may exhibit large differences. In general, intradural lesions were relatively small, whereas extradural lesions were larger; furthermore, the latter more easily formed an asymmetrical paraspinal soft tissue mass. In addition, of the four lesions in our series that presented with a "vault wall-like growth" pattern, three were extradural; of the five lesions that showed vertebral or other bone destruction, three were extradural. Thus, spPNETs located in different regions (intra- or extradural) appear different on images.

The first-line treatment for spPNET is a multimodal treatment strategy that consists of surgery, neo-adjuvant or adjuvant chemotherapy or radiotherapy. Although GTR of the tumor

is suggested as a cornerstone of therapy (19), most patients show recurrence or metastasis after the initial surgical treatment, and some studies found that this strategy did not significantly improve prognosis (7,16). Indeed, according to a previous report, more than 57% of patients died within 3 years (13). Neo-adjuvant therapy (i.e., preoperative radiotherapy and chemotherapy) has recently been found to significantly enhance survival, perhaps because this strategy shrinks the lesion, which facilitates GTR (2).

All but one patient in our series received GTR or STR of the tumor, followed by adjuvant chemotherapy, radiotherapy, or both. Six patients suffered from recurrence within two years. The survival period of the patients who underwent STR was shorter than that of the patients treated with GTR. One reason for this result might be that without total resection, a lesion easily recurs. Three of the four patients with lesions with a "vault wall-like growth" pattern accepted STR and exhibited a poor prognosis, with recurrence within 6 months and death within 24 months. We hypothesize that these lesions are more likely to invade surrounding structures, thereby resulting in a more difficult total resection. Given the small number of cases in our series, these findings should be confirmed by larger multi-institutional randomized control trials.

As mentioned above, it might be extremely difficult to differentiate spPNETs from other types of intraspinal tumors due to the lack of reliable imaging features (4,11). Schwannoma, the most difficult type of tumor to identify, is often accompanied by cystic degeneration, which is always located in the lesion center and shows hyper-intensity on T2-weighted images (12). Furthermore, schwannomas often lead to compressive bony absorption, whereas spPNET tends to present with bone destruction. Finally, although schwannomas often to grow through the neural foramen (as do spPNETs), its tendency to exhibit a "vault wall-like growth" pattern is not obvious, thus differing from spPNET. Overall, spinal meningiomas present with a broad and strong dural attachment as well as homogeneous enhancement, except in areas of calcification (20), though spinal meningiomas do not usually extend through the neural foramen. Lymphoma is a common extradural lesion that is difficult to differentiate from spPNET (20); this condition also often presents with an isointense signal on T1-weighted images and an isointense signal on T2-weighted images. However, lymphoma is usually found in middle-aged and older individuals and is rare in children younger than 10 years old. Lymphoma is also more likely to cause bone destruction but often lacks necrosis and hemorrhage. In addition, the characteristic of an extradural extension through the intervertebral foramen in lymphoma might be less evident than in spPNET. Extradural spPNETs are also differentiated from other extradural tumors (e.g., metastasis, multiple myeloma, chordoma, Ewing's sarcoma and eosinophilic granulomas) (20).

We acknowledge that the number of cases in this study is small, and this likely affected the reliability of our conclusions to some extent. An additional study with a large series of cases is necessary to provide sound evidence for the conclusions drawn in the present study.

CONCLUSION

Based on our findings, spPNETs have specific imaging characteristics, and our results differ from those of previous studies. spPNETs tend to occur at the sacrum level, often present with an isointense signal on T1-weighted images, show a "drilling hole" pattern, and might exhibit a "vault wall-like growth" pattern and an obvious linear enhancement pattern in certain cases. When accompanied by positive expression of Ki-67, hemorrhage and necrosis might not be rare features of spPNET. Obvious differences in the size, morphological features and rate of bone invasion between intradural and extradural lesions were observed. In addition, a positive association between Ki-67 expression and obvious hemorrhage, necrosis and bone destruction was detected in patients with spPNETs. If a spinal mass with the features described above is encountered in the clinic, spPNET should be added to the list of differential diagnoses.

ACKNOWLEDGEMENTS

Dr. Xiaoping YI is currently a Postdoctoral Fellow at the Postdoctoral Research Workstation of Pathology and Pathophysiology, Basic Medical Sciences, Xiangya Hospital, Central South University (No.185705). We also thank all the members of the Department of Radiology, XiangYa Hospital for helpful discussions. This study was supported by XiangYa-Peking University WeiMing Clinical and Rehabilitation Research Fund (No. xywm2015I35).

REFERENCES

1. Ba L, Tan H, Xiao H, Guan Y, Gao J, Gao X: Radiologic and clinicopathologic findings of peripheral primitive neuroectodermal tumors. Acta Radiol 56:820-828, 2015
2. Biswas B, Agarwala S, Shukla NK, Deo S, Sharma D, Thulkar S, Vishnubhatla S, Bakhshi S: Evaluation of outcome and prognostic factors in thoracic primitive neuroectodermal tumor: A study of 84 cases. Ann Thorac Surg 96:2006-2014, 2013
3. Duan XH, Ban XH, Liu B, Zhong XM, Guo RM, Zhang F, Liang BL, Shen J: Intraspinal primitive neuroectodermal tumor: Imaging findings in six cases. Eur J Radiol 80:426-431, 2011
4. Gebauer GP, Farjoodi P, Sciubba DM, Gokaslan ZL, Riley LH, Wasserman BA, Khanna AJ: Magnetic resonance imaging of spine tumors: Classification, differential diagnosis, and spectrum of disease. J Bone Joint Surg Am 90:146-162, 2008
5. Harimaya K, Oda Y, Matsuda S, Tanaka K, Chuman H, Iwamoto Y: Primitive neuroectodermal tumor and extraskeletal Ewing sarcoma arising primarily around the spinal column. Spine 28: E408-E412, 2003
6. Hou W, Sun X, Yin Y, Cheng J, Zhang Q, Xu J, Li Y, Zhou W, Wu H: Improving image quality for lung cancer imaging with optimal monochromatic energy level in dual energy spectral computed tomography. J Comput Assist Tomogr 40:243-247, 2016
7. Hrabálek L, Kalita O, Svebisova H, Ehrmann J, Hajduch M, Trojanec R, Kala M: Dumbbell-shaped peripheral primitive neuroectodermal tumor of the spine-case report and review of the literature. J Neurooncol 92:211-217, 2009

8. Hung SC, Lu YJ, Lin SC, Ho DMT, Guo WY, Chang CY: Imaging characteristics of primary spinal primitive neuroectodermal tumors. A report of five cases and literature review. Neuroradiol J 25:604-609, 2012
9. Jain A, Jalali R, Nadkarni TD, Sharma S: Primary intramedullary primitive neuroectodermal tumor of the cervical spinal cord. Case report. J Neurosurg Spine 4:497-502, 2006
10. Jingyu C, Jinning S, Hui M, Hua F: Intraspinal primitive neuroectodermal tumors: Report of four cases and review of the literature. Neurol India 57:661-668, 2009
11. Khanna AJ, Shindle MK, Wasserman BA, Gokaslan ZL, Gonzales RA, Buchowski JM, Riley LH 3rd: Use of magnetic resonance imaging in differentiating compartmental location of spinal tumors. Am J Orthop (Belle Mead NJ) 34:472-476, 2005
12. Koga H, Matsumoto S, Manabe J, Tanizawa T, Kawaguchi N: Definition of the target sign and its use for the diagnosis of schwannomas. Clin Orthop Relat Res 464:224-229, 2007
13. Mawrin C, Synowitz HJ, Kirches E, Kutz E, Dietzmann K, Weis S: Primary primitive neuroectodermal tumor of the spinal cord: Case report and review of the literature. Clin Neurol Neurosurg 104:36-40, 2002
14. Musahl V, Rihn JA, Fumich FE, Kang JD: Sacral intraspinal extradural primitive neuroectodermal tumor. Spine J 8:1024-1029, 2008
15. Otero-Rodríguez A, Hinojosa J, Esparza J, Muñoz MJ, Iglesias S, Rodríguez-Gil Y, Ricoy JR: Purely intramedullary spinal cord primitive neuroectodermal tumor: Case report and review of the literature. Neurocirugía 20:381-386; discussion 386-387, 2009
16. Qi W, Deng X, Liu T, Hou Y, Yang C, Wu L, Fang J, Tong X, Yang J, Xu Y: Comparison of primary spinal central and peripheral primitive neuroectodermal tumors in clinical and imaging characteristics and long-term outcome. World Neurosurg 88: 359-369, 2016
17. Tan Y, Zhang H, Ma GL, Xiao EH, Wang XC: Peripheral primitive neuroectodermal tumor: Dynamic CT, MRI and clinicopathological characteristics - analysis of 36 cases and review of the literature. Oncotarget 5:12968-12977, 2014
18. Thoriya PJ, Watal P, Bahri NU, Rathod K: Primary spinal primitive neuroectodermal tumor on MR imaging. Indian J Radiol Imaging 25(4):459-463, 2015
19. Tong X, Deng X, Yang T, Yang C, Wu L, Wu J, Yao Y, Fu Z, Wang S, Xu Y: Clinical presentation and long-term outcome of primary spinal peripheral primitive neuroectodermal tumors. J Neurooncol 124:455-463, 2015
20. Van Goethem JWM, van den Hauwe L, Ozsarlak O, De Schepper AMA, Parizel PM: Spinal tumors. Eur J Radiol 50: 159-176, 2004
21. Wu G, Ghimire P, Zhu L, Baral A, Su J: Magnetic resonance imaging characteristics of primary intraspinal peripheral primitive neuroectodermal tumour. Can Assoc Radiol J 64: 240-245, 2013
22. Zhang Y, Cai P, Chen M, Yi X, Li L, Xiao D, Liu W, Li W, Li Y: Imaging findings of adrenal primitive neuroectodermal tumors: A series of seven cases. Clin Transl Oncol 19:641-649, 2016